Geotechnical Aspects of Underground Construction in Soft Ground – Viggiani (ed)
© 2012 Taylor & Francis Group, London, ISBN 978-0-415-68367-8

Effects of the excavation procedure on the stability of diaphragm wall panels

D. L'Amante & A. Flora
Department of Hydraulic, Geotechnical and Environmental Engineering, University of Napoli Federico II, Napoli, Italy

ABSTRACT: The stability of panels during construction must be always considered in the design of diaphragm walls. The classical 2D methods to evaluate the maximum depth of excavation of a trench with or without slurry are too conservative for panels, because of the unrealistic geometrical simplification. Trying to back analyze a failure observed in Napoli during the excavation of a panel in a weakly cemented soil without slurry support, it was found that the position of the operating machine on the edge of the panel is likely to have played a role in the mechanism. Therefore, 2D and 3D FEM parametric numerical analysis have been carried out, to consider some relevant aspects that are generally neglected at the design stage, such as the real 3D geometry of the panels and the position of the operating machine. By comparing the FEM results with available 2D and 3D analytical solutions, it is found that the machine can play both a positive and a negative role on the stability of the panel, depending on its position.

1 INTRODUCTION

Deep excavations in urban area have to be realized minimizing the effects on the environment of all the working activities. The first to be considered is the construction of the retaining structure itself, both in terms of displacements of the soil and stability of the excavation (typically a panel). The panel can be realized with or without the use of stabilizing slurries, depending on soil physical and mechanical properties.

Adopting a limit equilibrium method (LEM), analytical solutions originally developed for trenches considering slurry pressure (Nash and Jones, 1963, Morghenstain and Thamasseb, 1965) are often used for stability calculations. In the case of a self sustaining material with no slurry, a simple solution is available considering the soil as a perfectly plastic material. In fact, the static and kinematic theorems state that the critical height h_c (*i.e.* the one corresponding to failure) is:

$$\frac{2c}{\gamma}\sqrt{K_p} \le h_c \le \frac{4c}{\gamma}\sqrt{K_p} \qquad (1)$$

where $K_p = \tan^2(45 + \varphi/2)$ is the passive coefficient of earth pressure.

For panels, which have a length of no more than a few meters, all these solutions result into an overconservative value of h_c because they refer to unrealistic plain strain (2D) conditions. More complex 3D LEM solutions can be used to take in account in a simple way the real geometry of the problem, even though all of them introduce arbitrary assumptions concerning the shape of the failure surface (Piaskowski & Kowalewski 1965, Fig. 1, Washbourne 1984, Fig. 2, Fox 2004 Fig. 3)

Since in 3D models the stabilizing forces increase with depth more rapidly than the destabilizing ones, the factor of safety may increase with depth, contrarily to what happens in the 2D models (Fig. 4). In this paper, the solutions of these 3D models are not reported for the sake of brevity. In the following, however, the solution by Fox (2004) (formally very long) will be used.

Nowadays, 2D and 3D numerical analyses are easily carried out to evaluate the stability of a panel, and are a reliable alternative to more traditional LEM formulas Lachler *et al.* (2007) and Brzakala and Gorska (2008) show a comparison between the factor of safety (3D) computed by LEM and FEM for slurry panels in cohesionless soils. In both cases the difference between the safety factors FS computed by LEM and by FEM is less than 25% of the largest value.

Lachler *et al.* (2007) also observe that FS decreases until a certain depth, after which it remains constant: for excavations deeper than this limit depth, the sliding wedge does not start at the bottom of the panel.

This paper reports the results of 2D and 3D FEM analyses, initially carried out to interpret a failure mechanism observed on a site by the authors and shortly recalled in the following. The

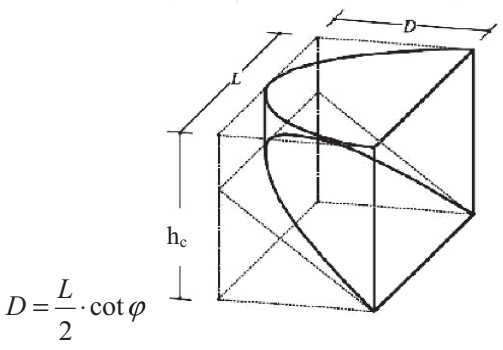

Figure 1. Unstable wedge (Piaskowski & Kowalewski, 1965) behind a panel having length L.

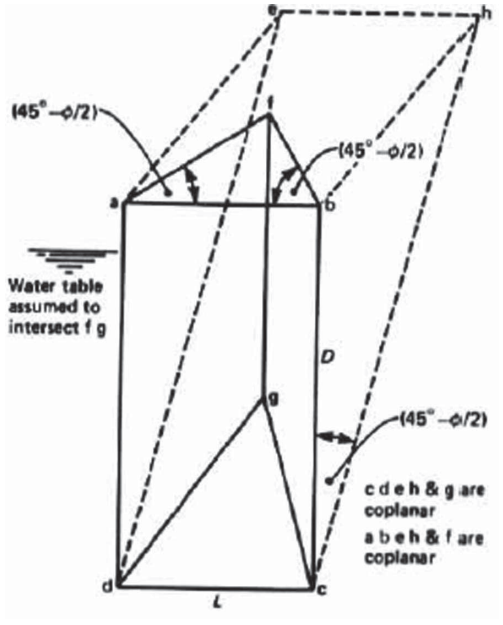

Figure 2. Unstable wedge behind a panel (Washbourne, 1984).

failure mechanism pertained to a panel excavated in a pyroclastic silty sand which, as shown in the next section, was expected to be stable considering the value of its critical height h_c calculated using LEM 3D formulas.

2 THE CASE HISTORY OF A PANEL COLLAPSED DURING CONSTRUCTION

For the construction of an underground parking lot in Napoli to be excavated in unsaturated pyroclastic silty sands (pozzolana), a sustaining

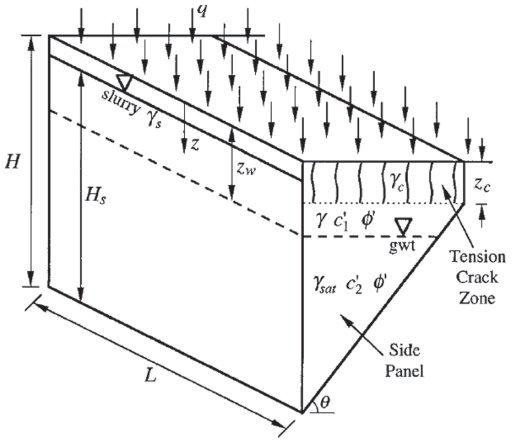

Figure 3. Unstable wedge behind a panel (Fox, 2004).

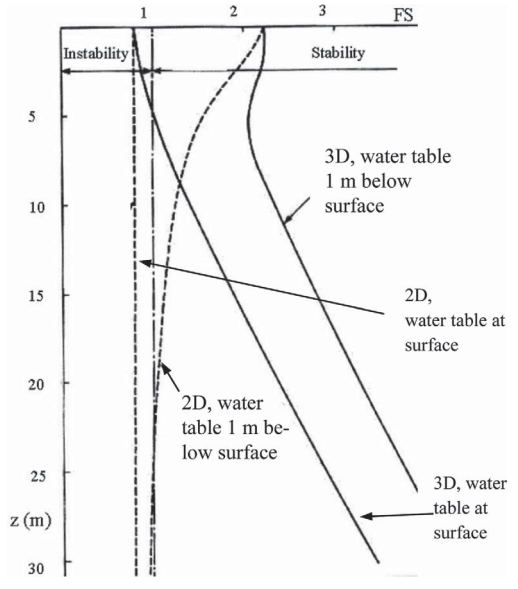

Figure 4. Safety factor FS versus depth for a 3D LEM solution (Washbourne, 1984).

structure consisting of a reinforced concrete diaphragm wall had to be realized. The wall is made of adjacent rectangular panels, 25 m deep and with a cross section of 6×0.6 m^2. For the unsaturated pozzolana, the geotechnical characterization reported an apparent cohesion $c = 10 \div 15$ kPa and a friction angle $\varphi = 35°$, being $\gamma = 12$ kN/m^3. These values are typical for simplified total stress analyses in these Neapolitan unsaturated materials. The designer decided to excavate the panels with no slurry support, assuming that soil cohesion was sufficient for stability, even though no stability calculation was included in the design report. Indeed, the application of the solution by Fox (2004) (Fig. 5) shows

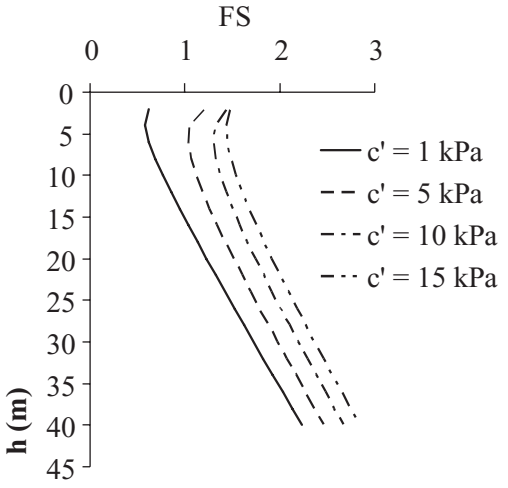

Figure 5. FS versus depth for different values of cohesion calculated using the solution by Fox (2004).

that for 10 kPa < c < 15 kPa, the excavation should be always stable, with a safety factor increasing with depth for z larger than about 6 m.

Unexpectedly, one of the first panels to be realized collapsed during the excavation (Fig. 6) at a depth of about 11 m, with a steep failure surface closed at middle depth of the panel under construction. The only difference with the other few panels previously realized without any problem was the position of the operating machine (Fig. 7), in this case placed on the longer side of the cross section of the panel. A numerical analysis was therefore planned to see if the position of the operating machine could be the factor explaining the observed failure mechanism, as described in the following section. However, before realizing the subsequent panels, ground improvement of the first few meters along the perimeter of the panels to be excavated was carried out. No other accident happened and the diaphragm wall was successfully completed.

3 NUMERICAL ANALYSES

The parametric numerical analyses were carried out with Plaxis 2D and Plaxis 3D Foundation. Four 2D and thirty-two 3D analyses have been carried out changing soil cohesion, panels dimensions and position of the operating machine. Three different positions of the operating machine have been considered in the 3D analyses: no machine (*absent load*), machine operating on the short side (*positive load*), machine operating on the long side (*negative load*). The first case is certainly unrealistic but is the one typically considered in both LEM and FEM solutions. The other two cases (positive and

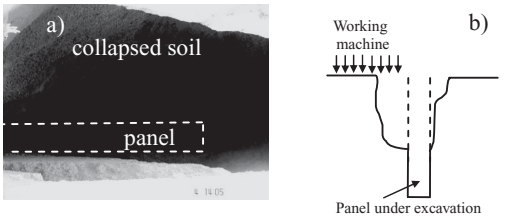

Figure 6. Collapsed panel. a) picture of the failure surface; b) sketch of the observed failure mechanism.

Figure 7. Pictures from the site in Napoli: different positions of the operating machine during panel excavation: a) on the long side; b) on the short side.

negative position of the machine) refer to positions that are both possible on site, as reported in the previous section.

In the calculations, the machine load is applied to the soil by a couple of belts. For each position, a different symmetry is adopted to prepare the mesh (Fig. 8). In 2D analyses, no machine load at ground level was considered.

Excavation has been simulated removing the soil in the panel by steps of 1 m, until the soil eventually collapse at a critical depth h_c.

For 3D analyses, in the case of absent load (double symmetry), the mesh is 100 m deep and 50×50 m^2 large, being composed by about 23000 wedge elements (Fig. 9). In the case of positive or negative load (simple symmetry) the volume of the mesh and the number of the elements is doubled. The 2D mesh is 100 m deep and 50 m large, composed by about 8000 triangular elements. All the meshes are finer around the panel.

The soil has been modeled using the Hardening Soil Model (HSM); the most relevant parameters for the mechanisms under study are reported in Tab. 1, with values of the cohesion between 1 and 15 kPa. The chosen values are typical of an uncemented unsaturated pozzolana.

Table 1. Main parameters of the soil in the FEM analyses.

γ_{sat} [kN/m^3]	ϕ' [°]	c′ [kPa]	Dilation angle, ψ [°]	K_0
12	35	1, 5, 10, 15, 20	5	0,9

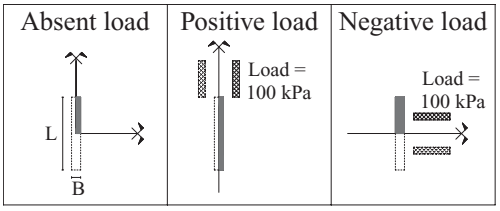

Figure 8. Position of the belt of the operating machine respect the panel and considered symmetry.

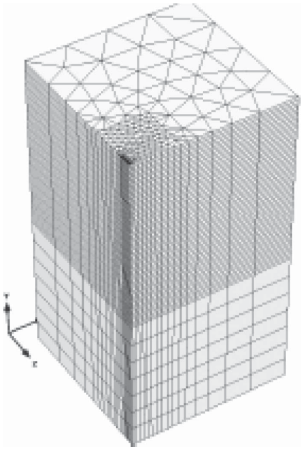

Figure 9. 3D mesh for the case of absent load.

4 ANALYSES OF RESULTS

Soil was assumed to collapse when the numerical analyses did not converge. With Plaxis, the sliding surface can be identified using several variables (shear strain, incremental shear strain, relative shear stress, plastic points). All of them were taken into account in this work. Tab. 2 reports a summary of the results obtained with 3D analyses. In the table, L and B and respectively the length and the width of the panel (Fig. 8).

In Fig. 10 some the 3D sliding surfaces for different values of cohesion in absence of load are shown for the case of panels having a cross section of 8×1 m^2. The horizontal cross section of these failure surfaces is approximately an arch of circumference having the side of the panel as a chord. The vertical section orthogonal to the long side of the panel shows the well known fact that these surfaces become steeper as cohesion increases; for $c' = 15$ kPa, the failure surface is mostly vertical (Fig. 10). For $c' = 20$ kPa, the analyses were stopped at a depth of excavation of 56 m without reaching failure.

For low values of the cohesion, the load of the operating machine plays a relevant role, influencing the value of the critical height h_c as well as the failure mechanism, which is deeply modified by the machine and resembles that typical of a foundation limit load failure (Figs. 11 and 12). For higher values of cohesion, the slip surface does not include the operating machine if the load is in a positive position.

Tab. 2 shows that, for conditions similar to those pertaining to the site in which the failure was observed and a negative position of the operating machine, the critical height h_c has values between 3 m and 26 m for cohesions in the range 5 kPa < c < 10 kPa, considering a panel having L = 6 m and B = 1 m. Even though this value of B is larger than the one on site, when the machine is on the long side of the excavation and the failure mechanism does not include the short side, the value of B is not very relevant. For the same panel, the cases of absent or positive load correspond to larger values of h_c. The depth of failure observed on site is consistent with the results of the analyses considering the operating machine in a negative position, thus confirming the relevance of this apparently minor load on the overall stability of the panel under excavation.

The results of 2D analyses are summarized in Tab. 3; in the table, both the critical excavation depth h_c and the depth of the bottom of the slip surface are reported. These results, as most of the 3D ones, show that the slip surface does not start from the bottom of the excavation (as supposed by LEM) but 1 or 2 meters above, consistently with the evidence recorded on site in Napoli (see previous section).

Table 2. 3D analyses carried out and resulted h_c.

B (m)	L (m)	Position	c′ (kPa)	h_c (m)
0,4	6	absent	10	33
0,4	8	absent	1–5–10–15	8–12–19–34
0,4	10	absent	10	15
0,4	12	absent	10	13
1	6	absent	5–10	14–32
1	8	absent	1–5-10–15	5–10–18–34
1	10	absent	10	14
1	12	absent	10	12
0,4	6	positive	10	33
0,4	8	positive	10	19
0,4	10	positive	10	14
0,4	12	positive	10	12
1	6	positive	5–10	13–36
1	8	positive	1–5–10–15	2–4–18–38
1	10	positive	10	14
1	12	positive	10	13
1	6	negative	5–10	3–26
1	8	negative	1–5–10–15	2–2–4–33
1	10	negative	10	3
1	12	negative	10	3

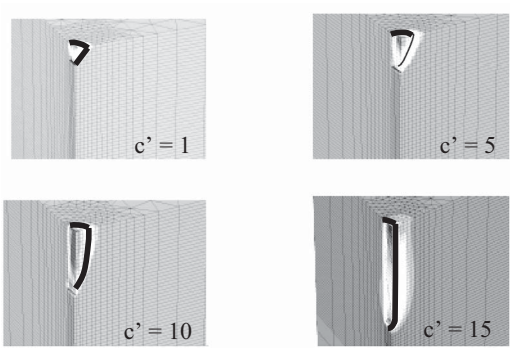

Figure 10. Sliding surface for different values of cohesion (incremental shear strain shadings, light color corresponds to the maximum value).

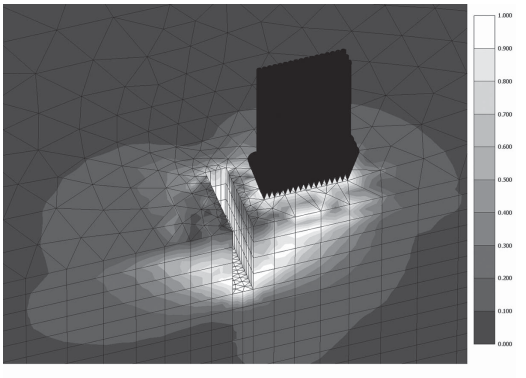

Figure 11. Unstable soil in the case of load in a negative position (τ/τ_{max} shading, light color correspond to the maximum value of relative shear stress) for c′ = 10 kPa, L = 8 m, B = 1 m.

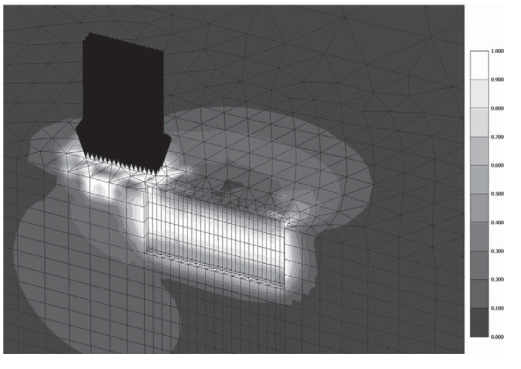

Figure 12. Unstable soil in the case of load in a positive position (τ/τ_{max} shading, light color correspond to the maximum value of relative shear stress) for c′ = 5 kPa, L = 8 m, B = 1 m.

Table 3. 2D analyses carried out and resulted h_c.

c′ (kPa)	1	5	10	15
h_c (m)	3	3	4	6
depth of failure mechanism (m)	1.7	2.7	3.7	5

Table 4. FS calculated with the formula of Fox (2004) for the critical heights h_c.

c′ (kPa)	h_c (m) (3D FEM)	FS (FOX, 2004)
1	5	0.60
5	10	1.12
10	18	1.66
15	34	2.55

In Tab. 4 the 3D results for the cases of absent load are summarized along with the extension D (see Fig. 1) of the failure surface at ground level calculated with some 3D LEM formulas and estimated in the numerical analyses. The value of D calculate with the approach of Washborne (1984) is the closest to FEM solutions; the solution by Piaskowski and Kowalewski (1965) overestimates D, while the one by Fox (2004) overestimates D for the deepest critical heights and underestimates it for the lowest ones.

In Fig. 13 the value of h_c calculated with 3D FEM is plotted versus c′ for different positions of the load (considering a panel having a cross section of 8×1 m^2). In the same figure, the values of h_c calculated by 2D LEM (Eq. 1) and 2D FEM are also reported. In the case of absence of load, h_c computed by FEM 3D is always larger than the one by 2D LEM and 2D FEM, and rapidly increases with c′.

Generally speaking, 2D and 3D FEM analyses give values of h_c smaller than the correspondent LEM, except for the case of a very low value of cohesion (c′ = 1 kPa). Fig. 13 also shows that, for 3D FEM analyses, for small values of cohesion the maximum value of h_c corresponds to the case of absence of load; somehow unexpectedly, on the contrary, for high values of the cohesion the machine may have a positive effect, the deepest possible excavation (largest value of h_c) corresponding to the case of operating machine on the short side of the panel (load in a positive position).

This can be physically explained by looking to the failure surface: for low values of cohesion (see Figs. 11 and 12) its position is influenced by the machine, which is all included in the unstable wedge of soil. When the cohesion is high, the much steeper failure surface has a position unaffected by the operating machine; in the case of positive

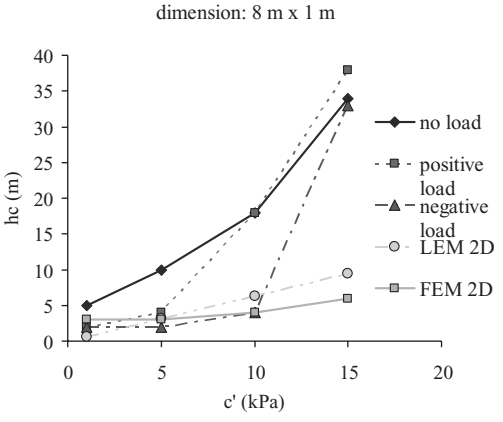

Figure 13. Value of h_C versus c′ and the position of the load.

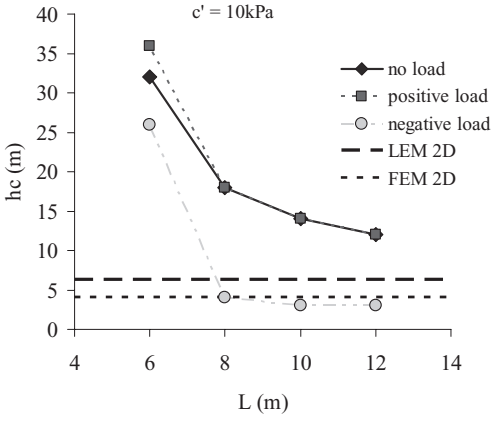

Figure 14. Value of h_c versus panel length L.

Table 5. Results for absent load: h_c calculated by 3D FEM; D by 3D LEM and 3D FEM.

L (m)	B (m)	c′ (kPa)	h_c (m)	H* (m)	D (m)	$D_{Washbourne}$ (m)	$D_{Piaskowski}$ (m)	D_{Fox} (m)
6	0,4	10	33	32	2	2,59	4,29	6,10
8	0,4	1	8	6	3,2	2,59	5,72	1,25
8	0,4	5	12	9	4,3	3,46	5,72	2,89
8	0,4	10	19	16	4,8	3,46	5,72	4,65
8	0,4	15	34	32	2,2	3,46	5,72	7,32
10	0,4	10	15	12,5	5	4,32	7,15	4,09
12	0,4	10	13	11	5,2	4,75	8,57	3,76
6	1	10	32	31	2	2,59	4,29	6,01
8	1	1	5	3	2	1,30	5,72	0,96
8	1	5	10	8,5	4	3,46	5,72	2,58
8	1	10	18	16	4,4	3,46	5,72	4,50
8	1	15	34	32	2,5	3,46	5,72	7,07
10	1	10	14	12	4,9	4,32	7,15	3,90
12	1	10	12	9,5	5,1	4,10	8,57	3,55

*depth of the slip surface.

load, the machine placed on the short side of the panel has the beneficial effect of increasing the mean stress within the soil, thus resulting into an increase of the critical height.

Fig. 14 reports the value of h_c versus panel length L for the different positions of the load, in the case of c′ = 10 kPa and B = 1 m. As expected, h_c decreases as L increases. In the case of negative load, for L > 8 m h_c becomes smaller than that calculated in 2D conditions. The cases with no load or with the load in a positive position have more or less the same h_c, the largest values pertaining to the latter case for the lower values of L.

In the case of load in negative position, h_c is always lower than in the other cases. For L higher than 10 m, h_c does not change. This is because

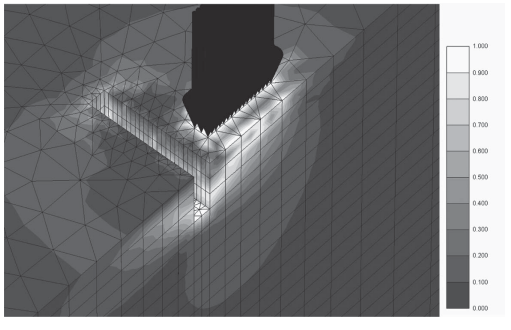

Figure 15. Unstable soil in the case of load in a negative position (τ/τ_{max} shading, light color correspond to the maximum value of relative shear stress), for c′ = 10 kPa, L = 12 m, B = 1 m.

as the length of the panel becomes large enough, the failure surface closes around the machine (Fig. 15), again resembling a foundation limit load mechanism, being unaffected by the remaining part of the panel, that therefore plays no role in the mechanism.

5 CONCLUSIONS

The stability of panels is a key issue in the design of diaphragm walls. A somehow unexpected failure mechanism observed on site by the authors during panel excavation with no slurry support in a weakly cemented material could be explained by taking into account the weight of the operating machine. To confirm this hypothesis and to analyze the effect the this usually neglected load has on the stability of panels excavated in soils with a small cohesion, 3D numerical analyses were carried out, comparing the results with some of the available analytical solutions.

It was found that 2D solutions (LEM or FEM) are usually conservative, unless an operating machine on the long side of the panel is considered. In this case, as the panel gets longer or the cohesion gets smaller, 3D FEM solutions give values of h_c lower than any 2D calculation. In most cases, the operating machine on the short side of the panel under excavation has a positive effect.

REFERENCE

Brzakala, W. & Gorska K. 2008. On Stability Analysis of Slurry–Wall Trenches. *Plaxis Bulletin 24*.

Fox, P.J. 2004. Analitical solution for stability of slurry trench. *Journal of Geotechnical and Geoenvironmental Engineering*: 749–757.

Lächler, A.; Vermeer P.A. & Wehnert, M. 2007. Assessment of diaphragm wall stability and deformation. *Proceedings of the 14th European Conference on Soil Mechanics and Geotechnical Engineering, Vol. 2, Madrid, Spain*: 1055–1060.

Morgenstern, N. R. & Amir-Tahmasseb I. 1965. The stability of slurry trenches in cohesionless soils. *Geotechnique* 15, n 4: 387–395.

Nash, J.K.T. & Jones, G.K. 1963. The support of trenches using fluid mud. *Grouts and Drilling Muds in Engineering Practice, London*: 177–180.

Piaskowski, A. & Kowalewski, Z. 1965. Application of tixotropic clay suspensions for stability of vertical sides of deep trenches without strutting. *6th Int. Conf. SMFE, Montreal.* Vol.III: 526–529.

Washbourne, J. 1984. The three dimensional stability analysis of diaphragm wall excavation. *Ground Engineering* 17(4): 24–29.